Hindawi Publishing Corporation
Journal of Nanomaterials
Volume 2013, Article ID 104825, 6 pages
http://dx.doi.org/10.1155/2013/104825

Research Article

UV-Ozone Treatment on Cs_2CO_3 Interfacial Layer for the Improvement of Inverted Polymer Solar Cells

Yusheng Xin, Zixuan Wang, Lu Xu, Xiaowei Xu, Yang Liu, and Fujun Zhang

Key Laboratory of Luminescence and Optical Information of Ministry of Education, Beijing Jiaotong University, Beijing 100044, China

Correspondence should be addressed to Fujun Zhang; fjzhang@bjtu.edu.cn

Received 11 November 2012; Revised 24 December 2012; Accepted 4 January 2013

Academic Editor: Jian Wei

Inverted configuration polymer solar cells (IPSCs) were prepared by using Cs_2CO_3 modified indium tin oxide (ITO) substrates as cathode and MoO_3/Al as anode, ITO/Cs_2CO_3/P3HT:PCBM/MoO_3/Al. The interfacial Cs_2CO_3 layers were conducted with annealing treatment and different time UV-Ozone treatment. The power conversion efficiency (PCE) of IPSCs was improved to 1% when the UV-Ozone treatment time is 15 minutes, with the open-circuit voltage of 0.48 V, short-circuit current density of 5.4 mA/cm^2, and fill factor of 39%. The improvement of IPSCs should be attributed to the increased electron transporting and collection ability of Cs_2CO_3 layer induced by UV-Ozone treatment. The underlying mechanism of PCE improvement was discussed in terms of series and shunt resistance of cells induced by UV-Ozone treatment on Cs_2CO_3 layer, and the mole ratio of Cs to O of Cs_2CO_3 layer with different UV-Ozone treatment was investigated by scanning electron microscopy operating in the mode for in situ energy dispersive X-ray (EDX) spectra.

1. Introduction

Polymer solar cells (PSCs) have attracted more and more attention as next-generation solar cells, owing to their merits of flight weight, lower cost, and friendly environments [1–3]. The power conversion efficiency (PCE) of organic solar cells has undergone a more than tenfold increase from ~1.0% by Tang in 1986 to ~10% in 2012 announced by Heliatek GmbH [4]. Along with the PCE increase of PSCs, the stability of PSCs is another key parameter for its application. The conventional structure PSCs are commonly prepared on indium tin oxide (ITO) substrates or ITO coated with poly(3,4-ethylenedioxythiophene):poly(styrene sulfonate) (PEDOT:PSS) substrates as anode and low work function metals as top cathode [5, 6]. However, metals with low work function are not very stable as the top electrode due to their sensitivity to oxygen and moisture in air. In order to improve the stability of PSCs, inverted configuration PSCs were designed with low work function materials modified ITO as the transparent cathode and a high work function metal as anode, which could effectively avoid the device degradation induced by the contamination of metal cathodes. Liao et al. demonstrate a highly efficient inverted bulk heterojunction PSCs based on regioregular poly(3-hexylthiophene):[6,6]-phenylC61 butyric acid methyl ester ($PC_{60}BM$) with a low temperature annealed interfacial buffer layer, cesium carbonate (Cs_2CO_3). This approach improves the power conversion efficiency of IPSCs from 2.3% to 4.2% [7]. Recently, Shim et al. reported inverted tandem PSCs with two identical active layers comprising a donor (P3HT) and a fullerene derivative acceptor $PC_{60}BM$, and the PCE of inverted tandem PSCs arrives to about 2.1% [8]. The most commonly used material system for PSCs consists of conjugated polymers as the electron donor and fullerene derivatives as the electron acceptor materials, blended in a bulk heterojunction (BHJ) to overcome the strong excitonic behavior of photogenerated charge carriers. The interpenetrated network of the donor-acceptor blend in the BHJ structure provides charge separation and charge transportation properties for achieving high efficiency. It is imperative that a bicontinuous network with a domain width approximately twice that of the exciton diffusion length and a high donor/acceptor interface is formed, which favors the exciton dissociation and transport of the separated charges to

the respective electrode. The active layer could be easily prepared by spin coating, inkjet printing, spray coating, gravure coating, and roller casting, which makes them feasible for preparing large scale PSCs [9, 10]. The main factors limiting the PSCs and IPSCs performance could be summarized as follows [11–13]: (i) incomplete solar spectrum absorption, (ii) thermalization of hot carriers (or excitons) in the form of excess heat, (iii) chemical potential (thermodynamic) losses dictating that the photovoltage must be less than band gap (E_G) for relaxed carriers, (iv) radiative recombination during charge carrier transport, and (v) the presence of other nonradiative losses.

Some effective methods were carried out to improve the performance of PSCs, such as thermal treatment, solvent treatment, adding additives, and inserting ultrathin buffer layers [14–19]. Sun and coworkers reported that PCE of the IPSCs based on P3HT: indene-C_{70} bisadduct was improved from 5.80% for the device without the additive to 6.35% for the device with 3-hexylthiophene additive and to 6.69% with 3-methylthiophene additive [17]. Oo et al. successfully exploited solution processed, high electron mobility and highly transparent zinc tin oxide (ZTO) as electron transporting buffer layer in IPSCs of FTO/ZTO/P3HT:PCBM/WO_3/Ag. The PCE of 3.05% was achieved, which was attributed to a better electron transporting, hole blocking capacities, and reduced recombination probabilities at electron collecting electrode with ZTO layer [19]. Park and his coworkers reported a facile and effective treatment method for controlling the morphology of bulk heterojunction (BHJ) structured polymer-based solar cells (PSCs) using a gas-assisted spray (g-spray) technique [20]. In order to achieve highly efficient IPSCs, it is critical to improve the electron collection of modified ITO electrode as well as suppress its hole collection. For IPSCs, the order of the layers is reversed with the top metal electrode now being the hole collecting anode. Low work function metals or metal oxidation, such as calcium, ZnO or Cs_2CO_3, are typically used to modified ITO substrates, and higher work function metals or metal oxidation, such as silver, gold, or MoO_3/Al, are selected as top anode in the IPSCs [21–24]. In this paper, we investigated the different UV-Ozone treatment time on the buffer layer Cs_2CO_3 on the effect of IPSCs performance.

2. Experimental Details

The indium tin oxide (ITO) glass substrates (sheet resistance 15 Ω/□) were cleaned consecutively in ultrasonic baths containing acetone, ethanol, and deionized water and dried by high pure nitrogen gas. The cleaned ITO substrates were treated by UV-Ozone for 10 min. The Cs_2CO_3 was dissolved in 2-ethoxyethanol or deionized water with the concentration 1 mg/mL and then spin-coated onto the ITO substrates at the speed of 4000 rpm for 40 seconds. The ITO substrates coated with Cs_2CO_3 thin film were transferred to a hot plate and annealed at 150°C for 20 min. Parts of Cs_2CO_3-coated ITO subtractes were treated by UV-Ozone with different time. Polymer electron donor P3HT and electron acceptor $PC_{60}BM$ were dissolved in chloroform with concentration 20 mg/mL, respectively, and then blended together with the same weight ratio. The blended solution was spin coated on Cs_2CO_3 coated ITO substrates at the speed of 2000 rpm for 30 seconds. The substrates coated with active layers were transferred to a vacuum chamber, and a 5 nm thickness layer of MoO_3 was deposited on the active layer under 5×10^{-3} Pa vacuum. The film thickness was monitored by a quartz crystal microbalance. The aluminum (Al) cathode with the thickness of 100 nm and the active area about 0.1 cm^2 defined through foursquare shadow mask was evaporated under 5×10^{-3} Pa conditions. The prepared IPSCs (ITO/Cs_2CO_3/P3HT:PCBM/MoO_3(5 nm)/Al) were carried out postannealing treatment under 120°C for 10 min.

The absorption spectra were measured by Shimadzu UV-3101 PC spectrometer. The current-voltage characteristics of IPSCs were measured by a Keithley source meter 2410 in dark and under illumination at 100 mW/cm^2 by using a 150 W Xenon lamp. The morphology of thin films was characterized by scanning electron microscope (SEM). The schematic diagrams of inverted configuration polymer solar cells and its energy level alignment are shown in Figure 1.

3. Results and Discussion

The absorption spectra of P3HT, PCBM, pristine P3HT:PCBM, and annealed P3HT:PCBM film are shown in the Figure 2. The electron donor material P3HT has a relative large absorption range from 450 nm to 600 nm, and its absorption peak locates at 517 nm. The electron acceptor material PCBM has a strong absorption peak at 300 nm and a weak absorption range from 400 nm to 550 nm. The blended P3HT:PCBM films show a distinguished blue shift of absorption peak at 480 nm compared with 517 nm of neat P3HT films. After annealing treatment on the blended film by 120°C with 10 min, the main absorption peak shifts to the 510 nm, and a shoulder absorption peak at 603 nm was observed. The variation of blended P3HT:PCBM absorption spectra should be attributed to the increased order phase of P3HT induced by annealing treatment, which was demonstrated by our pervious works and other groups [25–28].

All the inverted configuration polymer solar cells have the same cell configuration of ITO/Cs_2CO_3/P3HT:PCBM/MoO_3/Al; the only difference of each cell is UV-Ozone treatment time on Cs_2CO_3 interfacial layer. It was reported that Cs_2CO_3 decomposes into stoichiometric Cs_2O doped with Cs_2O_2 during thermal evaporation [29]. Liao and coworkers reported that the work function of annealed Cs_2CO_3 layer decreases from 3.45 to 3.06 eV by ultraviolet photoelectron spectroscopy [30]. The work function reduction could be attributed to this doped cesium oxide that behaves as a n-type semiconductor, with a lower interface resistance than pristine Cs_2CO_3. The ITO/Cs_2CO_3 was used as cathode to collect electron from the active layer. The MoO_3/Al was used as anode to collect hole from the active layer. The insertion of MoO_3 layer was found to be critical to the device performance, effectively extracting holes to prevent the exciton quenching and reducing the interfacial resistance because of alignment of energy levels [31]. It was demonstrated that ultrathin MoO_3 layer may form a tunneling

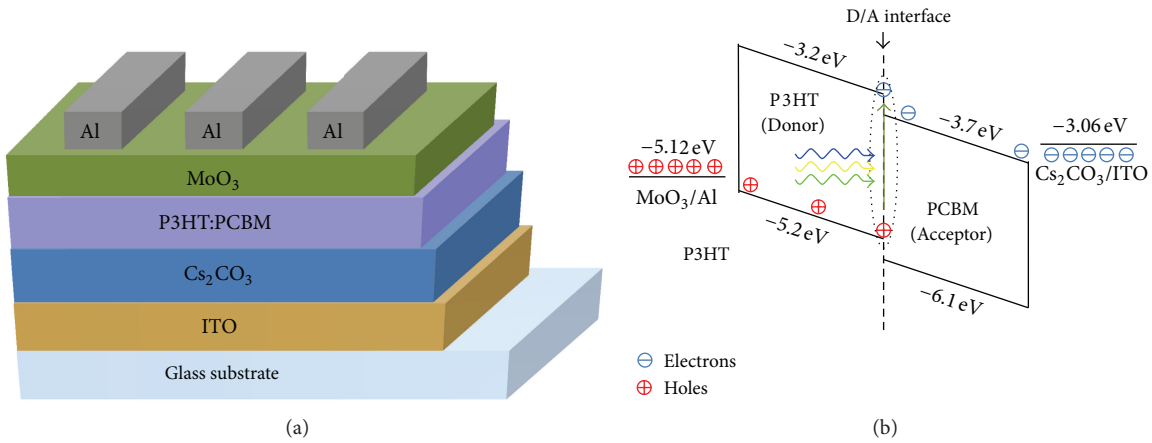

Figure 1: Schematic diagram of inverted configuration polymer solar cells and its energy level alignment.

Table 1: The key parameters of fabricated inverted polymer solar cells.

Number	Times	J_{sc} (mA/cm^2)	V_{oc} (V)	R_{sh} (Ω·cm^2)	R_s (Ω·cm^2)	FF %	PCE %
1	0 min	4.0	0.58	266	88	33	0.76
2	5 min	4.5	0.51	215	85	31	0.71
3	10 min	5.0	0.49	239	69	32	0.78
4	15 min	5.4	0.48	345	47	39	1.01
5	20 min	3.7	0.39	136	95	27	0.39

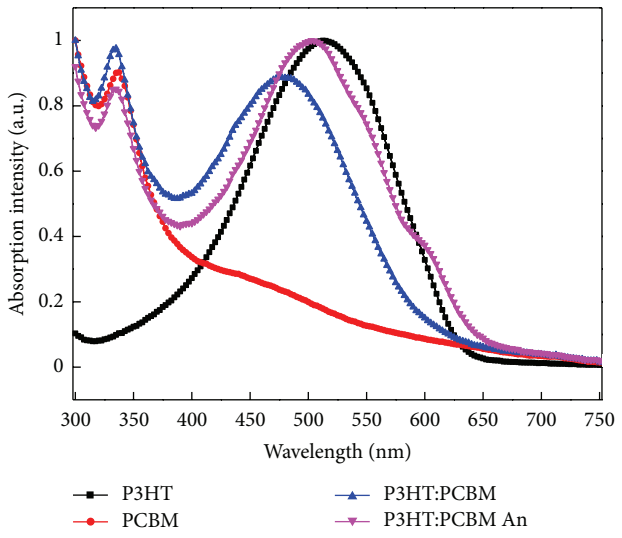

Figure 2: The absorption spectra of P3HT, PCBM, and the blended films.

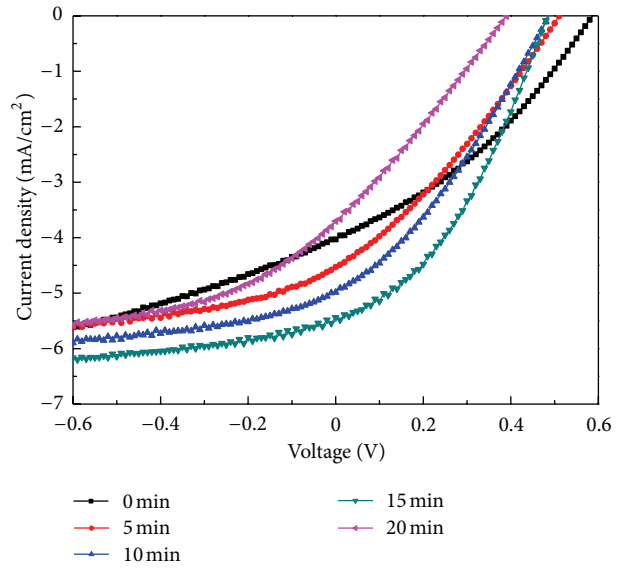

Figure 3: The *J-V* curves of IPSCs with different time UV-Ozone treatment on Cs_2CO_3 films under the illumination of 100 mW/Cm^2.

junction to increase built-in electric field, an interfacial dipole layer to shift the work function of electrodes [32]. The IPSCs *J-V* characteristic curves dependence on the UV-Ozone treatment time on Cs_2CO_3 under 100 mW/cm^2 are shown in the Figure 3. All the key parameters of IPSCs, including open circuit voltage (V_{oc}), short circuit current density (J_{sc}), fill factor (FF), power conversion efficiency (PCE), shunt resistance (R_{sh}), and series resistance (R_s), are summarized in the Table 1.

The V_{oc} was monotonously decreased along with increase of UV-Ozone treatment time on Cs_2CO_3 layer. However, the J_{sc} was firstly increased and then decreased when the UV-Ozone treatment time goes beyond 15 minutes. The maximum PCE of IPSCs arrives to 1% when the Cs_2CO_3 layer was treated by UV-Ozone with 15 minutes, which resulted from the increased J_{sc} and FF, the decreased V_{oc}. It is known

Table 2: Element analysis of Cs_2CO_3 film with different time of UV-Ozone treatment.

Elements		O	Si	In	Sn	Cs	O/Cs (mol)
5 min	Wt %	22.31	22.41	31.29	2.07	21.92	8.45
	At %	52.68	30.14	10.30	0.66	6.23	
10 min	Wt %	26.95	26.21	25.50	2.04	19.29	11.59
	At %	56.11	31.08	7.40	0.57	4.84	
15 min	Wt %	22.37	27.91	28.93	3.21	17.57	10.56
	At %	49.88	35.45	8.99	0.97	4.72	
20 min	Wt %	46.44	27.26	12.71	0.85	12.75	30.22
	At %	71.02	23.75	2.71	0.18	2.35	

(Wt %: weight percent; At %: elemental mol percent; O/Cs: Mol ratio.)

that the three parameters are very sensitive to the variation of series resistance (R_s) and shunt resistance (R_{sh}). The R_s of solar cells depends on resistance of the semiconductor bulk, the metal electrodes, and the metal/semiconductor interfaces. The R_s of cells is a parasitic, power consuming parameter. It decreases the maximum achievable output power, and hence it softens the *J-V* characteristics of a solar cell in the fourth quadrant. As seen from Table 1, the FF is also increased from 33% to 39% along with the decrease of R_s from 88 to 47 $\Omega\cdot cm^2$, which could be the enhancement of electronic coupling between the inorganic materials cesium oxides and active layer to mediate better forward charge transfer and reduce back charge recombination at the interface. The R_{sh} is relative to the recombination of charge carriers at the donor/acceptor interface and near electrodes. The R_{sh} was increased from 266 to 354 $\Omega\cdot cm^2$, which decreased the charge recombination between the buffer layer and the active layer interface. The combined effect of the decreased R_s and increased R_{sh} on charge carrier transport and collection results in the increase of J_{sc} and the reverse current saturation.

The dark *J-V* characteristic curves of all IPSCs are shown in Figure 4. All the IPSCs with Cs_2CO_3 layer undergoing UV-Ozone treatment have shown remarkable diodes prosperities, high forward current, and very low reverse current. However, there is a "S" shape *J-V* curve in the forward bias region for the cells based on Cs_2CO_3 layer without UV-Ozone treatment, resulting in the limit of charge carriers transport and collection. It is very apparent that the reverse dark current was markedly increased when the Cs_2CO_3 layer was UV-Ozone treatment about 20 minutes, and the high dark current in the reverse bias region can be attributed to the leakage current in reverse bias mode, resulting in much more charge carrier interfacial recombination and the decrease of short circuit current density.

Figure 5 shows the SEM images of ITO substrate and Cs_2CO_3 film on ITO substrates, and it is apparent that snowflake-like morphology of Cs_2CO_3 was observed. However, the Cs_2CO_3 films could not completely covered ITO surfaces when the Cs_2CO_3 films were prepared under the low spin coating conditions (500 rpm). In order to further confirm the effect of Cs_2CO_3 film modified ITO substrates on the performance of IPSCs. The elemental analysis of thick Cs_2CO_3 film with different treatments, annealing treatment,

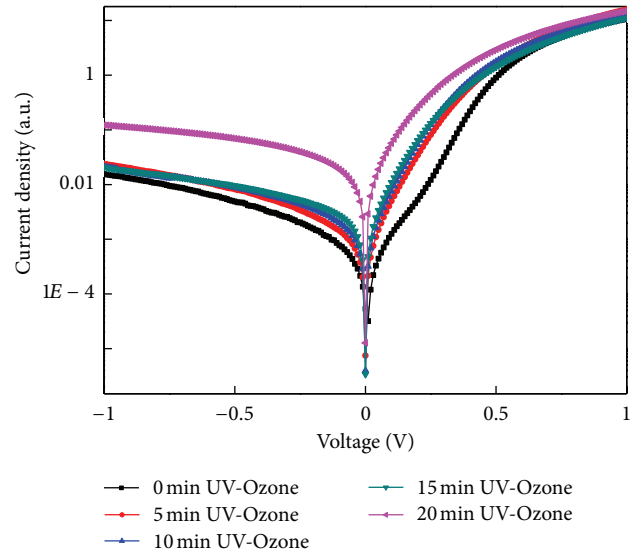

Figure 4: The *J-V* curves of IPSCs with different time UV-Ozone treatment on Cs_2CO_3 films in the dark.

and UV-Ozone treatment with different time was collected by SEM operating in the mode for in situ energy dispersive X-ray (EDX) spectra. The weight and mol percent of Si, O, Cs, In, and Sn elements were measured, and the mole ratio of O to Cs was summarized in the Table 2. The X-ray of In, Sn, O, and Si from ITO substrates could be collected due to the thin and discontinuous Cs_2CO_3 layer. Therefore, the relative ratio of Cs atom to O atom was simply discussed, which may be caused by UV-Ozone treatment on Cs_2CO_3 and the thickness of Cs_2CO_3 film and uncovered ITO surface.

4. Conclusions

A series of IPSCs based on the P3HT:PCBM as the active layer were fabricated with ITO/Cs_2CO_3 as cathode and MoO_3/Al as anode. The performances of IPSCs were enhanced when the Cs_2CO_3 layer was treated by UV-Ozone with 15 minutes, which should be attributed to the enhancement of carrier transport and collection by Cs_2CO_3 layer. The maximum PCE of IPSCs arrives to 1% with the open circuit voltage of 0.48V,

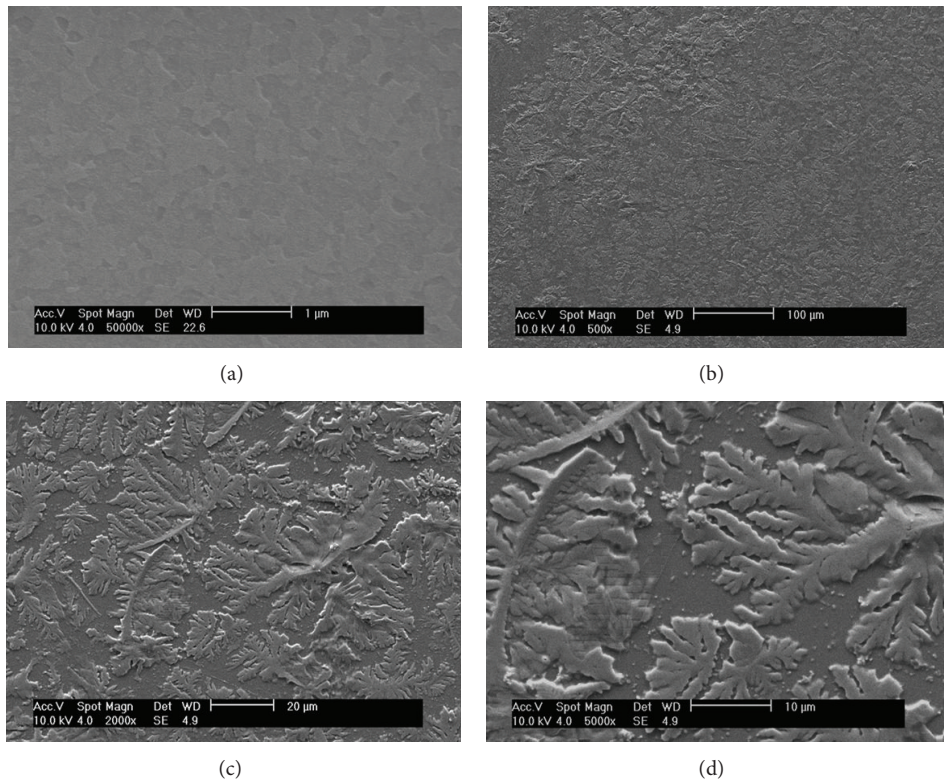

Figure 5: SEM pictures of (a) ITO surface, ((b)–(d)) Cs_2CO_3 films on ITO substrate with different magnification.

short circuit current density of 5.4 mA/cm^2, and fill factor of 39%.

Acknowledgments

The authors express their thanks to Beijing Natural Science Foundation (2122050); Basic Research Foundation of the Central Universities (2013JBZ004). F. Zhang thanks the support from the State Key Laboratory of Catalysis, CAS.

References

[1] N. J. Zhou, X. G. Guo, R. P. Ortiz et al., "Bithiophene imide and benzodithiophene copolymers for efficient inverted polymer solar cells," *Advanced Materials*, vol. 24, no. 17, pp. 2242–2248, 2012.

[2] H. Zhen, K. Li, Z. Huang et al., "Inverted indium-tin-oxide-free cone-shaped polymer solar cells for light trapping," *Applied Physics Letters*, vol. 100, no. 21, Article ID 213901, 2012.

[3] Y. Zhao, L. Zhu, J. Chen, and D. Ma, "Improving color stability of blue/orange complementary white OLEDs by using single-host double-emissive layer structure: comprehensive experimental investigation into the device working mechanism," *Organic Electronics*, vol. 13, no. 8, pp. 1340–1348, 2012.

[4] C. W. Tang, "Two-layer organic photovoltaic cell," *Applied Physics Letters*, vol. 48, no. 2, pp. 183–185, 1986.

[5] K. Sun, B. Zhao, V. Murugesan et al., "High-performance polymer solar cells with a conjugated zwitterion by solution processing or thermal deposition as the electron-collection interlayer," *Journal of Materials Chemistry*, vol. 22, no. 45, pp. 24155–24165, 2012.

[6] B.-Y. Ren, C.-J. Ou, C. Zhang et al., "Diarylfluorene-modified fulleropyrrolidine acceptors to tune aggregate morphology for solution-processable polymer/fullerene bulk-heterojunction solar cells," *Journal of Physical Chemistry C*, vol. 116, no. 16, pp. 8881–8887, 2012.

[7] H.-H. Liao, L.-M. Chen, Z. Xu, G. Li, and Y. Yang, "Highly efficient inverted polymer solar cell by low temperature annealing of Cs_2CO_3 interlayer," *Applied Physics Letters*, vol. 92, no. 17, Article ID 173303, 2008.

[8] J. W. Shim, Y. Zhou, C. Fuentes-Hernandez et al., "Studies of the optimization of recombination layers for inverted tandem polymer solar cells," *Solar Energy Materials and Solar Cells*, vol. 107, pp. 51–55, 2012.

[9] K. M. Coakley and M. D. McGehee, "Conjugated polymer photovoltaic cells," *Chemistry of Materials*, vol. 16, no. 23, pp. 4533–4542, 2004.

[10] F. Zhang, X. Xu, W. Tang et al., "Recent development of the inverted configuration organic solar cells," *Solar Energy Materials and Solar Cells*, vol. 95, no. 7, pp. 1785–1799, 2011.

[11] R. R. Lunt, T. P. Osedach, P. R. Brown, J. A. Rowehl, and V. Bulovic, "Practical roadmap and limits to nanostructured photovoltaics," *Advanced Materials*, vol. 23, no. 48, pp. 5712–5727, 2011.

[12] M. C. Hanna and A. J. Nozik, "Solar conversion efficiency of photovoltaic and photoelectrolysis cells with carrier multiplication absorbers," *Journal of Applied Physics*, vol. 100, no. 7, Article ID 074510, 2006.

[13] M. A. Green, K. Emery, Y. Hishikawa, and W. Warta, "Solar cell efficiency tables (version 37)," *Progress in Photovoltaics*, vol. 19, no. 1, pp. 84–92, 2011.

[14] B. Peng, X. Guo, C. Cui, Y. Zou, C. Pan, and Y. Li, "Performance improvement of polymer solar cells by using a solvent-treated poly(3,4-ethylenedioxythiophene):poly(styrenesulfonate) buffer layer," *Applied Physics Letters*, vol. 98, no. 24, Article ID 243308, 2011.

[15] J. S. Kim, W. S. Chung, K. Kim et al., "Performance optimization of polymer solar cells using electrostatically sprayed photoactive layers," *Advanced Functional Materials*, vol. 20, no. 20, pp. 3538–3546, 2010.

[16] S.-H. Chan, C.-S. Lai, H.-L. Chen, C. Ting, and C.-P. Chen, "Highly efficient P_3HT: C60 solar cell free of annealing process," *Macromolecules*, vol. 44, no. 22, pp. 8886–8891, 2011.

[17] Y. Sun, C. Cui, and H. Wang, "Efficiency enhancement of polymer solar cells based on poly(3-hexylthiophene)/indene-C_{70} bisadduct via methylthiophene additive," *Advanced Energy Materials*, vol. 1, no. 6, pp. 1058–1061, 2011.

[18] Z. Zhuo, F. Zhang, J. Wang et al., "Efficiency improvement of polymer solar cells by iodine doping," *Solid-State Electronics*, vol. 63, no. 1, pp. 83–88, 2011.

[19] T. Z. Oo, R. Devi Chandra, N. Yantara, R. R. Prabhakar, L. H. Wong, and S. G. Mhaisalkar, "Zinc Tin Oxide (ZTO) electron transporting buffer layer in inverted organic solar cell," *Organic Electronics*, vol. 13, no. 5, pp. 870–874, 2012.

[20] H. Y. Park, K. Kim, D. Y. Kim, S. K. Choi, S. M. Jo, and S. Y. Jang, "Facile external treatment for efficient nanoscale morphology control of polymer solar cells using a gas-assisted spray method," *Journal of Materials Chemistry*, vol. 21, no. 12, pp. 4457–4464, 2011.

[21] X. Xu, F. Zhang, J. Zhang et al., "High efficient inverted polymer solar cells with different annealing treatment," *Materials Science and Engineering C*, vol. 32, no. 4, pp. 685–691, 2012.

[22] F. J. Zhang, D. W. Zhao, Z. L. Zhuo, H. Wang, Z. Xu, and Y. S. Wang, "Inverted small molecule organic solar cells with Ca modified ITO as cathode and MoO_3 modified Ag as anode," *Solar Energy Materials and Solar Cells*, vol. 94, no. 12, pp. 2416–2421, 2010.

[23] X. W. Sun, D. W. Zhao, L. Ke, A. K. K. Kyaw, G. Q. Lo, and D. L. Kwong, "Inverted tandem organic solar cells with a MoO_3/Ag/Al/Ca intermediate layer," *Applied Physics Letters*, vol. 97, no. 5, Article ID 053303, 2010.

[24] A. K. K. Kyaw, X. W. Sun, C. Y. Jiang, G. Q. Lo, D. W. Zhao, and D. L. Kwong, "An inverted organic solar cell employing a sol-gel derived ZnO electron selective layer and thermal evaporated MoO_3 hole selective layer," *Applied Physics Letters*, vol. 93, no. 22, Article ID 221107, 2008.

[25] Z.-L. Zhuo, F.-J. Zhang, X.-W. Xu, J. Wang, L.-F. Lu, and Z. Xu, "Photovoltaic performance improvement of P_3HT:PCBM polymer solar cells by annealing treatment," *Acta Physico*, vol. 27, no. 4, pp. 875–880, 2011.

[26] C.-Y. Kuo, M.-S. Su, G.-Y. Chen, C.-S. Ku, and K.-H. Wei, "Annealing treatment improves the morphology and performance of photovoltaic devices prepared from thieno[3,4-c]pyrrole-4,6-dione-based donor/acceptor conjugated polymers and CdSe nanostructures," *Energy and Environmental Science*, vol. 4, no. 6, pp. 2316–2322, 2011.

[27] Z. Zhao, L. Rice, H. Efstathiadis, and P. Haldar, "Thickness dependent effects of thermal annealing and solvent vapor treatment of poly (3-hexylthiophene) and fullerene bulk heterojunction photovoltaics," in *MRS Fall Meeting, Photovoltaic Materials and Manufacturing Issues*, vol. 1123, pp. 171–178, December 2008.

[28] H.-Z. Yu and J.-B. Peng, "Annealing treatment effect on photoelectric properties of P_3HT:PCBM blend system," *Acta Physico*, vol. 24, no. 5, pp. 905–908, 2008.

[29] J. Huang, Z. Xu, and Y. Yang, "Low-work-function surface formed by solution-processed and thermally deposited nanoscale layers of cesium carbonate," *Advanced Functional Materials*, vol. 17, no. 12, pp. 1966–1973, 2007.

[30] H.-H. Liao, L.-M. Chen, Z. Xu, G. Li, and Y. Yang, "Highly efficient inverted polymer solar cell by low temperature annealing of Cs_2CO_3 interlayer," *Applied Physics Letters*, vol. 92, no. 17, Article ID 173303, 2008.

[31] F. Cheng, G. Fang, X. Fan et al., "Enhancing the short-circuit current and efficiency of organic solar cells using MoO_3 and CuPc as buffer layers," *Solar Energy Materials and Solar Cells*, vol. 95, no. 10, pp. 2914–2919, 2011.

[32] F. Zhang, F. Sun, Y. Shi et al., "Effect of an ultra-thin molybdenum trioxide layer and illumination intensity on the performance of organic photovoltaic devices," *Energy and Fuels*, vol. 24, no. 7, pp. 3739–3742, 2010.